



Supplementary Information for

Single-molecule analysis of actin filament debranching by cofilin and GMF

Johnson Chung¹, Bruce L. Goode^{2,#}, and Jeff Gelles^{1,#}

¹ Department of Biochemistry, Brandeis University, Waltham, MA 02454

² Department of Biology, Brandeis University, Waltham, MA 02454

Corresponding authors: gelles@brandeis.edu; goode@brandeis.edu

This PDF file includes:

Figures S1, S2, S3, S4, and S5

Tables S1 and S2

Legends for Movies S1 to S7

SI References

Other supplementary materials for this manuscript include the following:

Movies S1 to S7

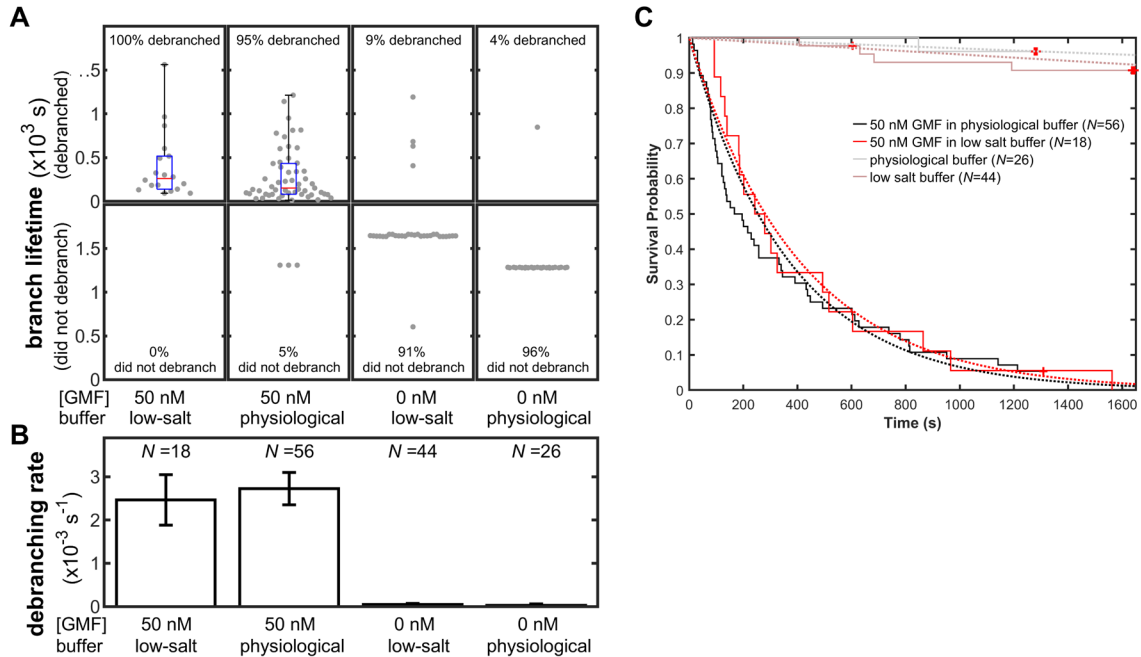


Figure S1: GMF induces debranching equally well in low-salt buffer and in physiological buffer. Experiments were conducted in low-salt or physiological buffer with zero or 50 nM GMF. (A) Points indicate lifetimes of individual branches seen to debranch (upper graph) or total time of observation for branches that lasted until the end of the experiment or diffused away without being seen to debranch (lower graph), Whisker plots indicate median (red), 25th and 75th percentiles (blue), and maximum and minimum (black). (B) Debranching rates (\pm SE) calculated from the data in (A). Calculation is based on both measured branch lifetimes and the total observation times for branches not seen to debranch (see *Materials and Methods*). Rates are summarized in SI Table S2. Measurement at 50 nM GMF in physiological buffer is the same as that shown in Figure 3. (C) Kaplan-Meier survival plots of data in (A) overlaid with single exponential curves using rate constants calculated in (B). Red crosses mark censored lifetime measurements.

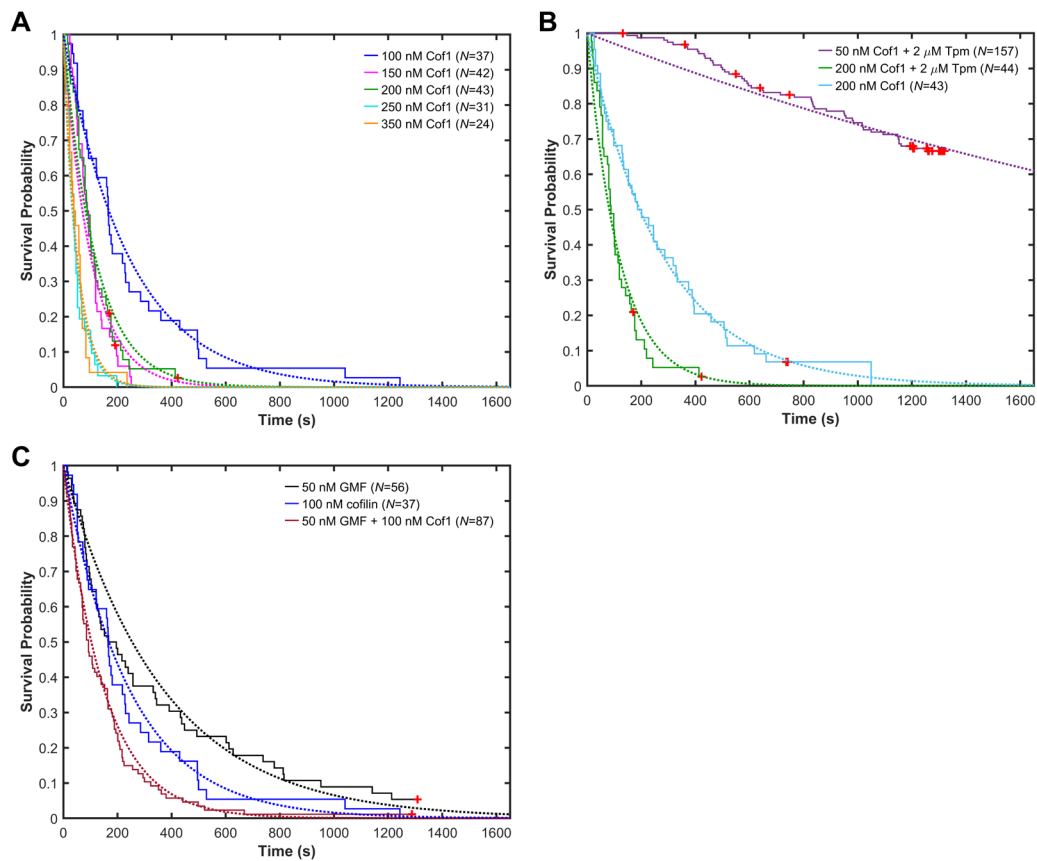


Figure S2: Survival distributions of branch lifetimes at various cofilin concentrations are exponential. Kaplan-Meier survival plots of branch lifetimes in physiological buffer, overlaid with exponential curves using rate constants shown in SI Table S2. Red crosses mark censored lifetime measurements. Lifetime measurements are from Figure 2B (A, B) and Figure 3 (C). 50 nM GMF data is the same as in Fig. S1 and is shown here for comparison.

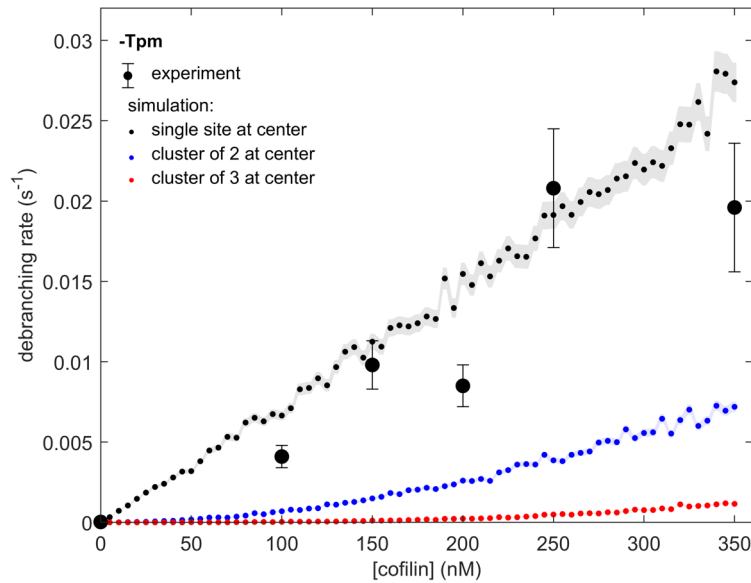
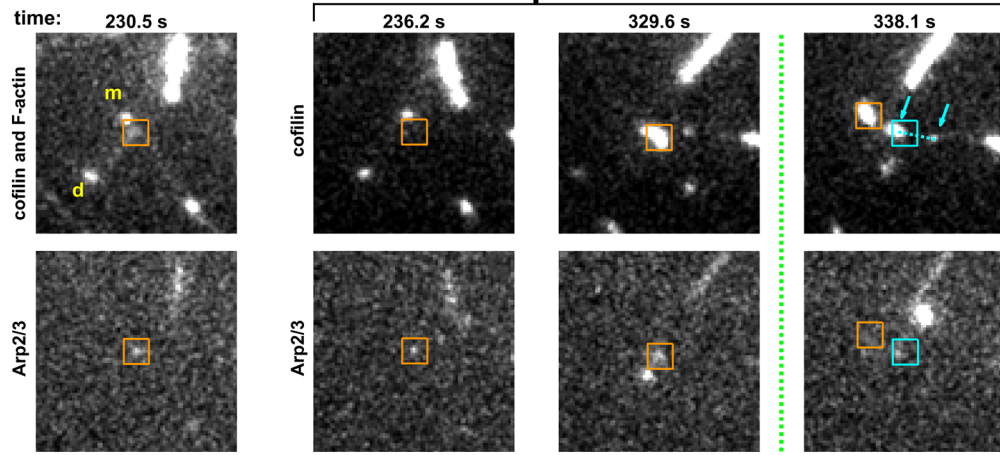
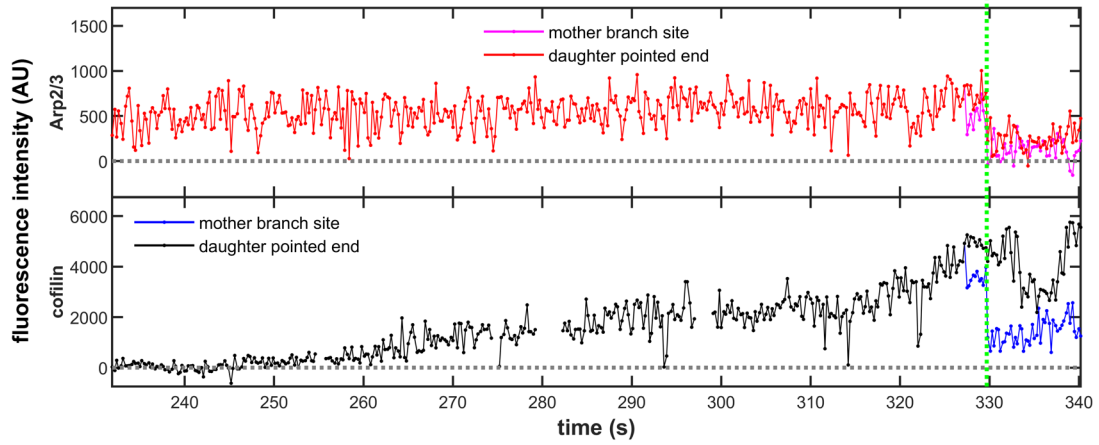


Figure S3: Comparison of observed debranching rates with model predictions. Debranching rates measured at different cofilin concentrations (black circles) from Fig. 2B overlaid by rates predicted from different mechanistic models of cofilin-induced debranching. Models assume that debranching is triggered by binding of a single cofilin molecule to a particular single actin subunit (black points), or to two consecutive subunits (blue points) or 3 consecutive subunits (red points) in the middle of a filament, in contrast to the end-binding models shown in Fig. 2C. Only the first model is consistent with the experimental data. Note that models are not fit to the data; each is a prediction with no free parameters calculated (see *Materials and Methods*) from the known cofilin binding/dissociation rate constants (1). Shading shows the SE of the model predictions.

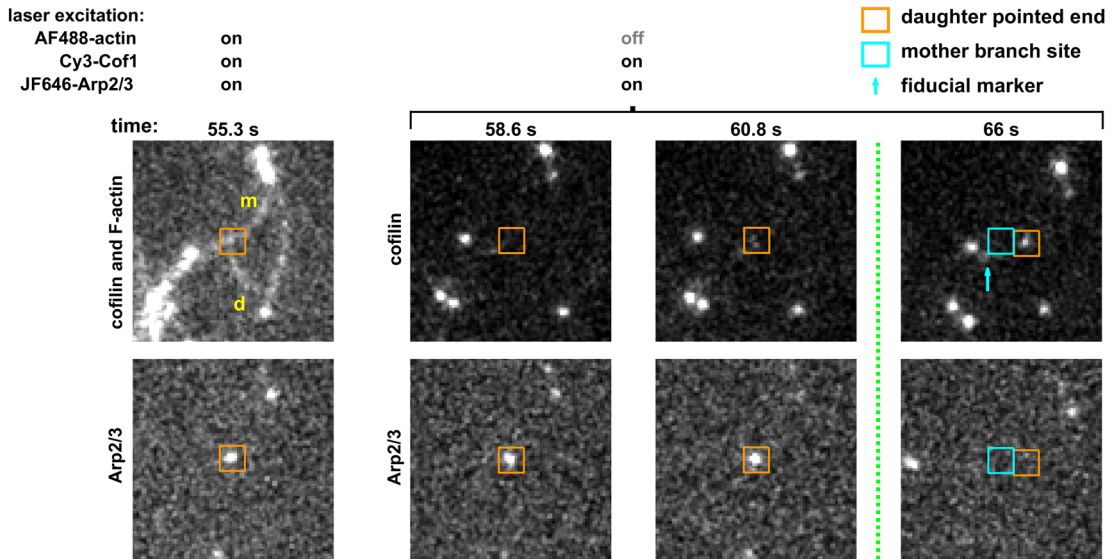
A

laser excitation: AF488-actin on off
 Cy3-Cof1 on on
 JF646-Arp2/3 on on

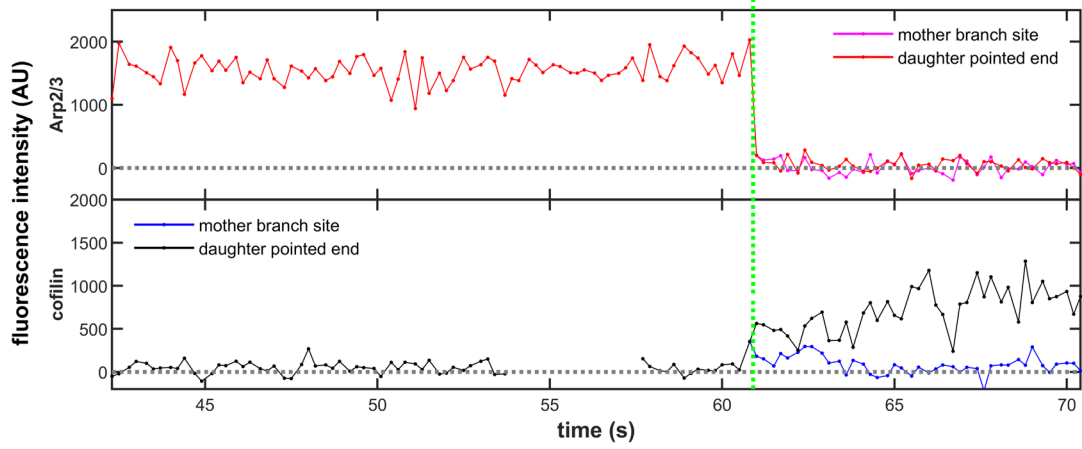
daughter pointed end
 mother branch site
↑ fiducial marker

**B**

C



D



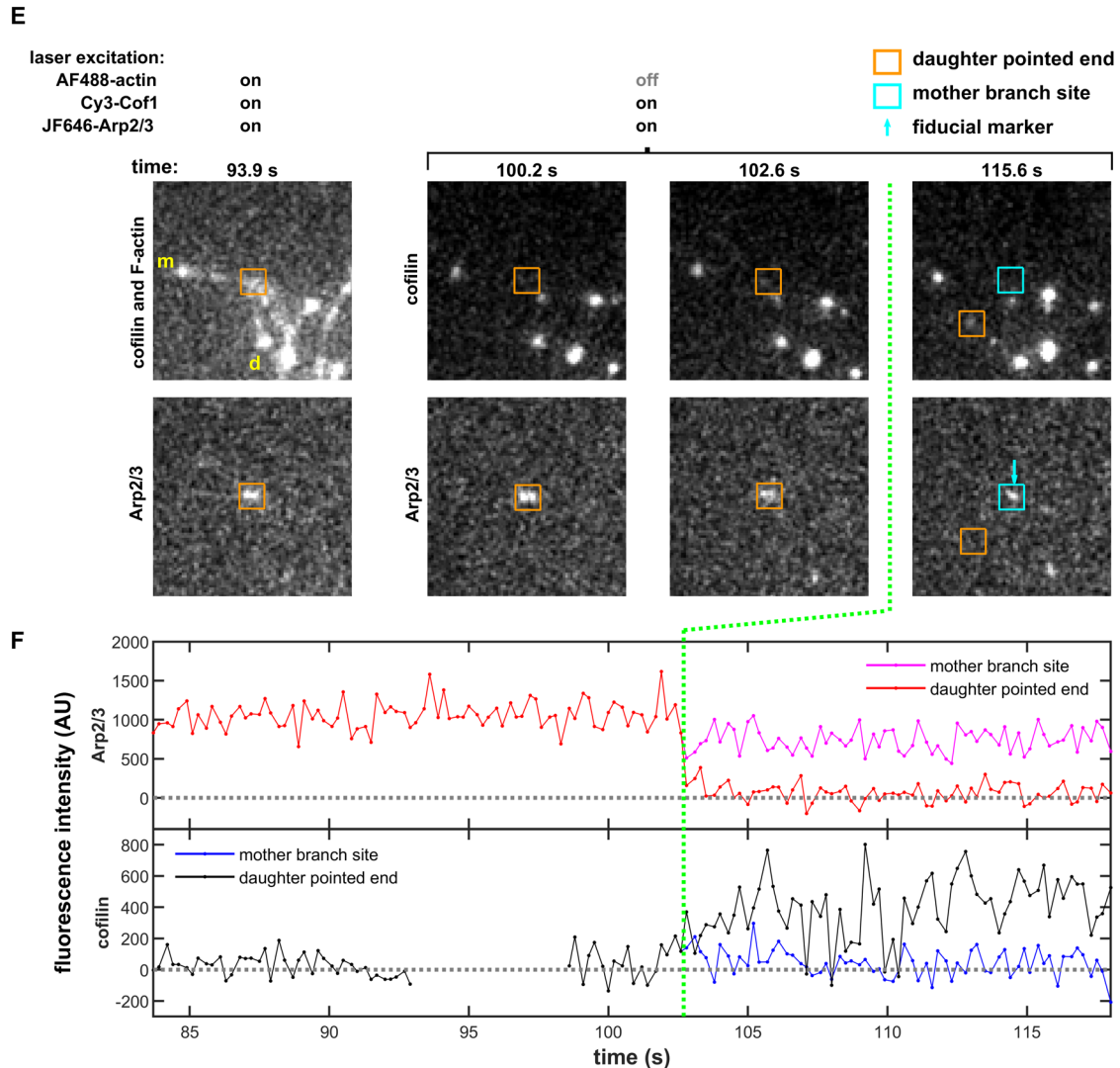


Figure S4: Additional example observations of labeled cofilin and Arp2/3 complex during debranching in the presence of 2 μ M Tpm1.7. (A,B), (C,D), and (E,F) show three examples, in addition to that in Fig. 4, of debranching events in physiological buffer. Each example is plotted as described for Fig. 4 and is taken from a different experimental replicate. These same three examples are also shown in Movies S2, S3, and S4, respectively. In these experimental records, interruptions in the cofilin recording are intervals when the AF488-actin excitation laser was briefly turned on to check the positions of the filaments. Post-debranching positions of the mother filament former branch site and daughter filament pointed end were determined as described in *Materials and Methods* using the indicated fiducial marks (arrows) and subsequent F-actin images. A $9.7 \mu\text{m} \times 9.7 \mu\text{m}$ area centered at the mother branch site of each image is displayed. The images displayed here were spatially filtered by a 2×2 matrix of ones to improve clarity.

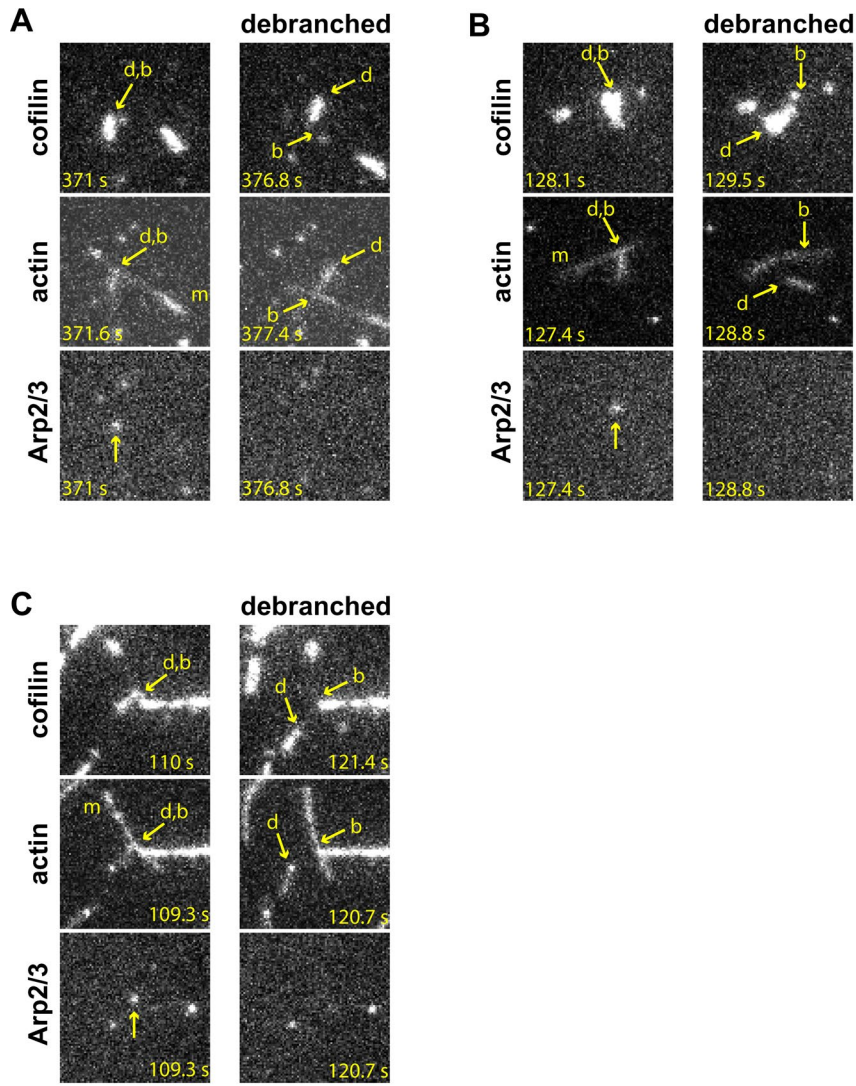


Figure S5: Images of labeled Arp 2/3 complex, cofilin, and actin taken immediately before (left) and after (right) debranching. Figure shows still images taken from Movie S5 (A), Movie S6 (B), and Movie S7 (C). Each image is $9.7 \mu\text{m} \times 9.7 \mu\text{m}$. Yellow arrows mark the daughter pointed end (d), and branch site on the mother filament (b) before and after debranching. The location of the mother filament (m) is indicated in the actin channel before debranching. The upward-pointing yellow arrows in the Arp2/3 images before debranching mark the Arp2/3 spots.

Table S1: Ionic composition of buffers and their support of debranching

	van Eunen buffer ^a	physiological buffer ^b	low-salt buffer ^c
<u>debranching by GMF</u>	<i>no</i>	<i>yes</i>	<i>yes</i>
<u>composition</u>			
K ⁺ (mM)	300	275	50
Na ⁺ (mM)	20	20	0
Mg ²⁺ (mM)	3	3	2
Ca ²⁺ (mM)	0.5	0	0
HEPES (mM)	0	50	50 ^d
pH	6.8	7.0	7.4
glutamate (mM)	245	245	0
Cl ⁻ (mM)	0	0	54
phosphate (mM)	50	0.001	0
sulfate (mM)	3	3	0
EGTA (mM)	0	0	1

^aYeast cytoplasmic ionic concentrations inferred from elemental analysis (2, 3). Preliminary experiments showed that this buffer did not support GMF-mediated debranching. Debranching in cytoplasm can presumably proceed because the inhibitory Ca²⁺ and P_i ions are sequestered in subcellular organelles (3, 4).

^bUsed in this paper. Prepared as a 3× stock by mixing 60 mM Na⁺•HEPES, 90 mM K⁺•HEPES, 735 mM K⁺•glutamate, 3 μM K₂HPO₄, 9 mM MgSO₄ and adjusting to pH 7 with acetic acid.

^cSimilar to buffers used in previous actin dynamics studies (5–9) except for the HEPES buffer to suppress pH changes due to O₂-scavenging (10, 11). Prepared as a 10× stock by mixing 500 mM HEPES, 20 mM MgCl₂, 500 mM KCl, 10 mM EGTA and adjusting to pH 7.4 with KOH.

^dImidazole was substituted for HEPES for the low-salt buffer experiments in Fig. 5 because HEPES buffer reduced the fluorescence of AF488-actin.

Table S2: Calculated rate constants for branch lifetime data sets^a

	debranching rate ^b		<i>N</i> _{total}	<i>N</i> _{debranched}
	s ⁻¹	S.E.		
50 nM GMF in low salt	0.0025	0.0006	18	18
50 nM GMF	0.0027	0.0004	56	53
low salt	4.8 × 10 ⁻⁵	2.4 × 10 ⁻⁵	44	4
physiological buffer	3.0 × 10 ⁻⁵	3.0 × 10 ⁻⁵	26	1
50 nM Cof1 + 2 μM Tpm	3.0 × 10 ⁻⁴	0.42 × 10 ⁻⁴	157	51
100 nM Cof1	0.0041	0.0007	37	37
150 nM Cof1	0.0098	0.0015	42	41
200 nM Cof1	0.0085	0.0013	43	41
200 nM Cof1 + 2 μM Tpm	0.0036	0.0005	44	42
250 nM Cof1	0.0208	0.0037	31	31
350 nM Cof1	0.0196	0.0040	24	24
50 nM GMF + 100 nM Cof1	0.0067	0.0007	87	86

^aMeasured in physiological buffer except where designated “low salt”

^bRates reported here are calculated as the Bayesian estimates (see *Materials and Methods*) and are identical to values derived using a maximum likelihood fitting method that accounts for censored data.

Legends for Movies S1 to S7

Movie S1: Example of a debranching event with fluorescently labeled cofilin and Arp2/3 complex in the presence of 2 μM Tpm1.7. Same event as depicted in Fig. 4. Time sequence of a $10.9 \mu\text{m} \times 10.9 \mu\text{m}$ area centered at the branch site (both before and after debranching). In this movie the green laser (exciting Cy3-Cof1) and red laser (exciting JF646-Arp2/3 complex) were on continuously; the blue laser (exciting AF488-actin) was on only during two brief intervals at the beginning and end of the movie, as indicated in the text overlay. The two fiducial markers (cyan arrows), Cy3-Cof1 accumulations at both ends of the mother filament, were used to infer the position of the former branch site on the mother filament after debranching. Images in the movie were spatially filtered by a 2×2 matrix of ones.

Movie S2: Example of a debranching event with fluorescently labeled cofilin and Arp2/3 complex in the presence of 2 μM Tpm1.7. Same event as depicted in Fig. S4 A and B. Time sequence of a $10.9 \mu\text{m} \times 10.9 \mu\text{m}$ area centered at the branch site (both before and after debranching). In this movie the green laser (exciting Cy3-Cof1) and red laser (exciting JF646-Arp2/3 complex) were on continuously; the blue laser (exciting AF488-actin) was on only during three brief intervals indicated in the text overlay. The two fiducial markers (cyan arrows), Cy3-Cof1 accumulations at one end and at middle of the mother filament, were used to infer the position of the former branch site on the mother filament after debranching. Images in the movie were spatially filtered by a 2×2 matrix of ones.

Movie S3: Example of a debranching event with fluorescently labeled cofilin and Arp2/3 complex in the presence of 2 μM Tpm1.7. Same event as depicted in Fig. S4 C and D. Time sequence of a $10.9 \mu\text{m} \times 10.9 \mu\text{m}$ area centered at the branch site (both before and after debranching). In this movie the green laser (exciting Cy3-Cof1) and red laser (exciting JF646-Arp2/3 complex) were on continuously; the blue laser (exciting AF488-actin) was on only during three brief intervals at the beginning, in the middle, and at the end of the movie, as indicated in the text overlay. The fiducial marker (cyan arrow), a Cy3-Cof1 accumulation on the mother filament near the branch site, was used to infer the position of the former branch site on the mother filament after debranching. Images in the movie were spatially filtered by a 2×2 matrix of ones.

Movie S4: Example of a debranching event with fluorescently labeled cofilin and Arp2/3 complex in the presence of 2 μM Tpm1.7. Same event as depicted in Fig. S4 E and F. Time sequence of a $10.9 \mu\text{m} \times 10.9 \mu\text{m}$ area

centered at the branch site (both before and after debranching). In this movie the green laser (exciting Cy3-Cof1) and red laser (exciting JF646-Arp2/3 complex) were on continuously; the blue laser (exciting AF488-actin) was on only during three brief intervals at the beginning, in the middle, and at the end of the movie, as indicated in the text overlay. The fiducial marker (cyan arrow), an Arp2/3 complex from a nearby branch on the same mother filament that did not debranch during this recording, was used to infer the position of the former branch site on the mother filament after debranching. Images in the movie were spatially filtered by a 2 x 2 matrix of ones.

Movie S5: Example of a debranching event in the presence of 2 μ M Tpm1.7 visualized with interleaved imaging of actin and Arp2/3+cofilin. Time sequence of a 10.9 μ m \times 10.9 μ m area centered at the branch site (both before and after debranching). Simultaneous red plus green excitation frames (JF646-Arp2/3 and Cy3-cofilin) were acquired in alternation with blue excitation frames (AF488-actin). The branch junction in the green channel before debranching was mapped from the Arp2/3 position in the red channel. The branch junction position along the mother filament contour just before debranching was used to infer the position of the former branch site on the mother filament after debranching. The locations of the pointed end of daughter filament in the green and blue channels after debranching were identified by inspection. Images in the movie were spatially filtered by a 2 x 2 matrix of ones.

Movie S6: Example of a debranching event in the presence of 0.2 μ M Tpm1.7 visualized with interleaved imaging of cofilin and actin+Arp2/3. Time sequence of a 10.9 μ m \times 10.9 μ m area centered at the branch site (both before and after debranching). Simultaneous red plus blue excitation frames (JF646-Arp2/3 and AF488-actin) were acquired in alternation with green excitation frames (Cy3-cofilin). The branch junction in the blue channel before debranching was mapped from the Arp2/3 position in the red channel. The branch junction position along the mother filament contour just before debranching was used to infer the position of the former branch site on the mother filament after debranching. The locations of the pointed end of daughter filament in the green and blue channels after debranching were identified by inspection. In this experiment a reduced (0.2 μ M) concentration of Tpm was used to allow more cofilin decoration of the filaments. Images in the movie were spatially filtered by a 2 x 2 matrix of ones.

Movie S7: Example of a debranching event in the presence of 0.2 μ M Tpm1.7 visualized with interleaved imaging of cofilin and actin+Arp2/3. A

second example of a debranching event imaged and analyzed in the same way as in Movie S6.

SI References

1. K. Hayakawa, S. Sakakibara, M. Sokabe, H. Tatsumi, Single-molecule imaging and kinetic analysis of cooperative cofilin–actin filament interactions. *Proc Natl Acad Sci USA* **111**, 9810–9815 (2014).
2. K. van Eunen, B. M. Bakker, The importance and challenges of in vivo-like enzyme kinetics. *Perspectives in Science* **1**, 126–130 (2014).
3. K. van Eunen, *et al.*, Measuring enzyme activities under standardized in vivo-like conditions for systems biology. *The FEBS Journal* **277**, 749–760 (2010).
4. T. Dunn, K. Gable, T. Beeler, Regulation of cellular Ca²⁺ by yeast vacuoles. *Journal of Biological Chemistry* **269**, 7273–7278 (1994).
5. L. Blanchoin, T. D. Pollard, R. D. Mullins, Interactions of ADF/cofilin, Arp2/3 complex, capping protein and profilin in remodeling of branched actin filament networks. *Curr Biol* **10**, 1273–1282 (2000).
6. M. Gandhi, *et al.*, GMF is a cofilin homolog that binds Arp2/3 complex to stimulate filament debranching and inhibit actin nucleation. *Curr Biol* **20**, 861–867 (2010).
7. C. A. Ydenberg, *et al.*, GMF Severs Actin-Arp2/3 Complex Branch Junctions by a Cofilin-like Mechanism. *Curr Biol* **23**, 1037–1045 (2013).
8. C. Chan, C. C. Beltzner, T. D. Pollard, Cofilin Dissociates Arp2/3 Complex and Branches from Actin Filaments. *Curr Biol* **19**, 537–545 (2009).
9. N. G. Pandit, *et al.*, Force and phosphate release from Arp2/3 complex promote dissociation of actin filament branches. *Proc Natl Acad Sci USA* **117**, 13519–13528 (2020).
10. X. Shi, J. Lim, T. Ha, Acidification of the oxygen scavenging system in single-molecule fluorescence studies: in situ sensing with a ratiometric dual-emission probe. *Anal. Chem.* **82**, 6132–6138 (2010).
11. B. A. Smith, *et al.*, Three-color single molecule imaging shows WASP detachment from Arp2/3 complex triggers actin filament branch formation. *Elife* **2**, e01008 (2013).